

AD-A081 148

NAVAL POSTGRADUATE SCHOOL MONTEREY CA  
EXPERIMENTAL STUDY OF THE RADIATION PROPERTIES OF A PARAMETRIC --ETC(U)  
SEP 79 S E TRENCHARD

F/B 20/1

AL

UNCLASSIFIED

1 OF 1

40  
209 148

END

DATE

FILED

3-80

DDI

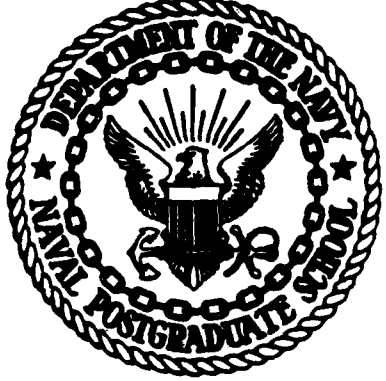
2

# NAVAL POSTGRADUATE SCHOOL

Monterey, California

ADA 081148

LEVEL



SDTIC  
ELECTED  
FEB 28 1980  
C

## THESIS

EXPERIMENTAL STUDY OF THE RADIATION  
PROPERTIES OF A PARAMETRIC FOG HORN

by

Stephen Edward Trenchard

September 1979

Thesis Advisor: A. B. Coppens

Approved for public release; distribution unlimited.

DDC FILE COPY

10 128

UNCLASSIFIED

SECURITY CLASSIFICATION OF THIS PAGE (When Data Entered)

REPORT DOCUMENTATION PAGE		READ INSTRUCTIONS BEFORE COMPLETING FORM
1. REPORT NUMBER	2. GOVT ACCESSION NO.	3. RECIPIENT'S CATALOG NUMBER
4. TITLE (and Subtitle) Experimental Study of the Radiation Properties of a Parametric Fog Horn		5. TYPE OF REPORT & PERIOD COVERED Master's Thesis September 1979
7. AUTHOR(s) Stephen Edward/Trenchard		6. PERFORMING ORG. REPORT NUMBER
8. PERFORMING ORGANIZATION NAME AND ADDRESS Naval Postgraduate School Monterey, California 93940		9. CONTRACT OR GRANT NUMBER(s)
11. CONTROLLING OFFICE NAME AND ADDRESS Naval Postgraduate School Monterey, California 93940		10. PROGRAM ELEMENT, PROJECT, TASK AREA & WORK UNIT NUMBERS
14. MONITORING AGENCY NAME & ADDRESS (if different from Controlling Office) 12759		12. REPORT DATE Sep 79 13. NUMBER OF PAGES 58
		15. SECURITY CLASS. (of this report) Unclassified
		16. DECLASSIFICATION/DOWNGRADING SCHEDULE
16. DISTRIBUTION STATEMENT (of this Report) Approved for public release; distribution unlimited.		
17. DISTRIBUTION STATEMENT (of the abstract entered in Block 20, if different from Report)		
18. SUPPLEMENTARY NOTES		
19. KEY WORDS (Continue on reverse side if necessary and identify by block number) Parametric Fog Horn Fog Signaling		
20. ABSTRACT (Continue on reverse side if necessary and identify by block number) An experimental study of the radiation properties of a parametric fog horn was conducted using a 4 unit x 5 unit horn driver array as the primary source. The horn was operated as two separate 10-unit acoustic arrays each transmitting one primary frequency. The frequency combinations studied were 4240-5520Hz and 4960-5520Hz. The acoustic properties of the parametric array were observed for both frequency combinations.		

(20. ABSTRACT Continued)

Source levels were varied between 122dB re 200Pa and 134dB re 200Pa at 1 meter to study the transition from absorption limited performance to saturation limited performance. Results consistent with the predictions of Moffett and Mellen [JASA 61, 325-337 (1977)] for the source level of the difference frequency beam and saturation broadening of the difference frequency beam were observed. The horn was also operated as a single array with all units radiating both primary frequencies. Equivalent results were obtained. A discussion of fog signaling applications is included.

Accession For	
NIDS C&I	<input checked="" type="checkbox"/>
DDO TAB	<input type="checkbox"/>
Unannounced	<input type="checkbox"/>
Justification	
By	
Distribution/	
Applicability Code	
Dist	Avail and/or special
A	

DD Form 1473  
 1 Jan 73  
 S/N 0102-014-6601

UNCLASSIFIED

2 SECURITY CLASSIFICATION OF THIS PAGE (When Data Entered)

Approved for public release; distribution unlimited.

Experimental Study of the Radiation  
Properties of a Parametric Fog Horn

by

Stephen Edward Trenchard  
Lieutenant, United States Coast Guard  
B.S., United States Coast Guard Academy, 1973

Submitted in partial fulfillment of the  
requirements for the degree of

MASTER OF SCIENCE IN PHYSICS

from the

NAVAL POSTGRADUATE SCHOOL

September 1979

Author

Stephen E. Trenchard

Approved by:

Charles B. Coppers Thesis Advisor

James V. Sanders Second Reader

John M. Dyer  
Chairman, Department of Physics and Chemistry

William M. Tolles  
Dean of Science and Engineering

### ABSTRACT

An experimental study of the radiation properties of a parameter fog horn was conducted using a 4 unit x 5 unit horn driver array as the primary source. The horn was operated as two separate 10-unit acoustic arrays each transmitting one primary frequency. The frequency combinations studied were 4240-5520Hz and 4960-5520Hz. The acoustic properties of the parameter array were observed for both frequency combinations. Source levels were varied between 122dB re 20 $\mu$ Pa and 134dB re 20 $\mu$ Pa at 1 meter to study the transition from absorption limited performance to saturation limited performance. Results consistent with the predictions of Moffett and Mellen [JASA 61, 325-337 (1977)] for the source level of the difference frequency beam and saturation broadening of the difference frequency beam were observed. The horn was also operated as a single array with all units radiating both primary frequencies. Equivalent results were obtained. A discussion of fog signaling applications is included.

TABLE OF CONTENTS

I.	INTRODUCTION -----	7
	A. BACKGROUND -----	7
	B. OUTLINE OF INVESTIGATION -----	8
	C. PERFORMANCE REQUIREMENTS -----	8
II.	PARAMETER SOURCE THEORY -----	10
	A. NEARFIELD MODEL -----	10
	B. FARFIELD MODEL -----	12
	C. COMPREHENSIVE MODEL -----	14
III.	EXPERIMENTAL PARAMETRIC SOURCE -----	20
	A. ARRAY CHARACTERISTICS -----	20
	B. PARAMETRIC OPERATION OF THE ARRAY -----	23
	1. Mixed Method -----	23
	2. Split Method -----	28
	C. TRANSMITTING EQUIPMENT -----	28
IV.	RECEPTION AND RECEIVING EQUIPMENT -----	30
	A. RECEPTION OF PARAMETRIC SIGNAL -----	30
	B. RECEIVING EQUIPMENT -----	31
	C. DATA ACQUISITION -----	35
	D. EQUIPMENT CHECKOUT AND CALIBRATION -----	36
V.	EXPERIMENTAL INVESTIGATION -----	38
	A. PROPAGATION -----	38
	B. SOURCE LEVEL DIFFERENCE VS. SOURCE LEVEL PRIMARY -----	42
	C. SPLIT AND MIXED TRANSMITTING -----	47

VI.	RESULTS AND CONCLUSIONS -----	50
A.	EXPERIMENTAL DATA AND THEORETICAL PREDICTIONS -----	50
B.	FOG SIGNALING CAPABILITY -----	51
C.	DISADVANTAGES OF PARAMETRIC SOURCE -----	54
D.	APPLICATIONS -----	54
	LIST OF REFERENCES -----	55
	INITIAL DISTRIBUTION LIST -----	57

## I. INTRODUCTION

### A. BACKGROUND

The U.S Coast Guard's shore-based sound-signal system includes over 600 signals, many of which are located near communities and residential areas. As part of its automation program the Coast Guard is replacing multifrequency air-driven sound signals with pure tone electric air oscillators. Installation of these pure tone oscillators has increased noise complaints of residents near the signals. One signal, the un baffled ELG300-02 (dual-emitter), is capable of producing levels of 80dB(A) as far as one half mile to the rear of the signal. Environmental Protection Agency guidelines state that 60DB(A) is the maximum level of a pure tone in urban areas. [1] To avoid complains levels of 50dB(A) or less are probably desirable in suburban and rural areas.

Bolt, Beneranek And Newman, Inc., developed and improved baffle for the ELG300-02 (dual emitter). The baffle design goal was attenuation of 30dB to 40dB to the rear in the dark sector of the signal. A baffle design featuring combined acoustically hard and soft surfaces was developed that provided 30dB of attenuation in the dark sector. [2] The improved baffle has two drawbacks: Its large size (10ft x 18ft) and its cost (\$10,000 each).

## B. OUTLINE OF INVESTIGATION

The purpose of this investigation was to test a model parametric source. A parametric source could ideally provide an acceptable sound level in the bright sector of the signal with little or no noise in the dark sector of the signal.

Previous work on the parametric array in air has been limited. Shealy did some initial work on parametric beam widths and directivity patterns. [3] Bennett did work on propagation of the difference frequency, however, primary source levels were not high (95dB to 105dB re 20 $\mu$ Pa), and the difference frequency was very weak (40dB to 50dB re 20 $\mu$ Pa). [4] Brinkman reported a difference frequency source level of 108dB re 20 $\mu$ Pa from primary source levels of 130dB re 20 $\mu$ Pa. [5] Brinkman's difference frequency was 10kHz which was too high for fog signaling applications. None of the previous experiments had been carried out to the farfield of the parametric array. Brinkman's single data point was the only one available to check the Moffett and Mellen design curves in air [6] and there is some question of how close Brinkman's point is to the predicted level. It was concluded that previous work on the parametric array in air was not sufficient to predict performance in fog signaling applications.

## C. PERFORMANCE REQUIREMENTS FOR FOG SIGNALING

A set of minimum performance criteria is proposed as a measure of the usefulness of the parametric array in air for fog signaling applications:

(1) Difference frequency greater than 100Hz but less than 1100Hz [7]

(2) Difference-frequency level greater than 120dB re 20 $\mu$ Pa giving a "usual range of detection" of the signal of one mile at 1100Hz [8]

(3) Significant reduction of noise from backward radiation (The baffle design goal of 30dB attenuation in the dark sector will be adopted.)

(4) Capability to steer the narrow difference-frequency beam over large angles.

## II. PARAMETRIC SOURCE THEORY

The interaction of two intense sound waves, called primary waves, of coincident direction of propagation and different frequencies results in the formation of combinational waves. The combinational waves propagate at frequencies equal to the sum and the difference of the primary wave frequencies. The difference-frequency wave, also called secondary pressure wave, has greater engineering application due to its property of high directionality at low frequency.

In 1963, Westervelt outlined the basic solution for the secondary pressure wave at the difference frequency. [9] The secondary pressure wave is assumed to be generated by a distributed volume of sources whose strengths depend on the local level of the primary waves. This volume source is termed the "parametric source." The spreading geometry and absorptive behavior of the primary waves in the interaction region has been the basis for different theoretical developments.

### A. NEARFIELD SOURCE

Westervelt's original theory dealt with the difference frequency signal generated from narrow, plane, collimated primary waves. It is the model for a parametric source constrained by absorption of the primary waves in the nearfields of the primary beams. The Rayleigh length,  $R_0$ , defines the transition range from the nearfield to the farfield of the

primary beams. The Rayleigh length is the ratio of the source area,  $A_o$ , to the mean primary wave length,  $\lambda_o$ .

$$R_o \equiv \frac{A_o}{\lambda_o} = \frac{A_o f_o}{c} \quad (2-1)$$

where  $f_o = \frac{f_1 + f_2}{2} =$  mean primary wave frequency.

Westervelt found a solution for the secondary pressure wave

$$P_d(r, \theta) = \frac{\beta \omega_d^2 P_1 P_2 A_o}{4\pi r \rho_o c^4 \alpha_T} \exp(-\alpha_d + jk_d)r D(\theta) \quad (2-2)$$

where

$r, \theta =$  field coordinates

$\beta =$  parameter on non-linearity = 1.2 for air

$\alpha_d =$  attenuation coefficient of secondary wave

$\alpha_{1,2} =$  attenuation coefficient of primary waves

$\alpha_T = \alpha_1 + \alpha_2 - \alpha_d$

$P_{1,2} =$  pressure of the primary waves

$\rho_o =$  density of medium

$c =$  speed of sound

$\omega_d =$  angular frequency of secondary wave

$k_d = \frac{2\pi}{\lambda_d}$  where  $\lambda_d$  is the difference frequency wavelength.

and

$$D(\theta) = \left( 1 + \left( \frac{2k_d}{\alpha_T} \right)^2 \sin^4 \frac{\theta}{2} \right)^{-1/2} \quad (2-3)$$

where  $D(\theta)$  is the directionality factor of the secondary wave.

The secondary wave is generated near the source wherever the product of the primary wave pressures  $P_1 P_2$  is large. Once generated the secondary wave propagates with its own attenuation appropriate to that frequency. The secondary sound pressure will be down 3dB at the angle  $\theta_d$  where

$$\sin \frac{\theta_d}{2} = \left( \frac{\alpha_T}{2k_d} \right)^{1/2} \quad (2-4)$$

if  $\alpha_T/k_d$  is small, the beam width of the secondary wave is

$$2\theta_d = \sqrt{\frac{2\alpha_T}{k_d}} \quad (2-5)$$

This secondary pressure wave is a narrow, nearly sidelobe-free beam of low frequency.

#### B. FARFIELD SOURCE

Berktay and Leahy extended Westervelt's model to a farfield source where the bulk of the interaction is assumed to take place at a distance greater than the Rayleigh length. [10] In this region the primary waves are assumed to spread spherically. Bertkay and Leahy chose to write the on-axis secondary pressure in terms of the acoustic power  $W_{1,2}$  of the primary waves where

$$W_{1,2} = A_o (P_{1,2})^2 / 2\rho_o c_o \quad (2-6)$$

The secondary pressure becomes

$$P_d(r,0) = \frac{\omega_d^2 W_1^{1/2} W_2^{1/2}}{2\pi c_o^3 r \alpha_T} e^{-(\alpha_d + jk_d)r} \quad (2-7)$$

Substituting the appropriate constants for air and writing  $\alpha_T$  in terms of  $\theta_d$ , the RMS value of  $P_d$  at 1 meter,

$$P_d(1,0) = \left[ \frac{2.4(180)^2}{\sqrt{2} \pi^2 3.44^2} \right] \frac{f_d W_1^{1/2} W_2^{1/2}}{\theta_d^2} \quad (2-8)$$

From this expression a preliminary design equation may be deduced as

$$SL_d = 127.5 + 20 \log f_d + 10 \log W_1 + 10 \log W_2 - 40 \log \theta_d + 20 \log |V| \quad (\text{dB re } 20 \mu P_a) \quad (2-9)$$

where  $f_d$  is in kHz,  $W_1, W_2$  are in watts,  $\theta_d$  is in degrees and  $20 \log |V|$  is a correction factor involving transducer geometry.

[10] A more convenient form of the design equation results from use of the source levels of the primary beams,

$$SL_i = 10 \log W_i + DI_i + 109 (\text{dB re } 20 \mu P_a) \quad (2-10)$$

In air this yields

$$\begin{aligned}
SL_D = & -90.5 + 20\log f_d + (SL_1 - DI_1) + (SL_2 + DI_2) \\
& - 40\log \theta_d + 20\log |V| \text{ (dB re } 20\mu P_a) \quad (2-11)
\end{aligned}$$

In a farfield source Westervelts beam width is only good for very narrow primary beams. If  $2\theta_d$  is much smaller than the product of the primary directivity functions, then  $D(\theta)$  becomes the product of the primary directivity functions.

### C. COMPREHENSIVE MODEL

There are two additional operating regimes for parameter sources. At high input powers the parametric array length becomes limited by nonlinear absorption. These arrays are called saturation limited, because their effective length is determined by saturation of the primary signal from the generation of harmonics and shock formation. Moffett and Mellen have developed a model which incorporates all four operating regimes of the parametric array. [6]

The on-axis secondary pressure for the comprehensive model is written

$$P_d(r, 0) = \frac{\pi \beta P_o^2 R_o f_d^2}{\rho c^3 f_o r} (I_1 + I_2) \quad (2-12)$$

where the integral  $I_1$  is a measure of the contribution from the collimated portion of the primary wave (Westervelt model) and the integral  $I_2$  is a measure of the contribution from the spherically spreading portion (Beektaay-Leahy model).

The source area,  $A_o$ , of Westervelt's model has been written

in terms of the Rayleigh length,  $R_0$ , the primaries have been assumed to have the same pressure,  $P_1 = P_2 = P_0$ , and frequency,  $f_0$ , and  $I_1$  and  $I_2$  are functions of  $\alpha_T$ .

The complex parameter gain is defined as the ratio of the on-axis secondary pressure amplitude to the amplitude of one primary

$$g \equiv rP_d(r,0)/P_0R_0 \quad (2-13)$$

Substituting  $P_d$  in yields

$$g = \frac{x}{2} \left( \frac{f_d}{f_0} \right)^2 \left( \frac{I_1 + I_2}{R_0} \right) \quad (2-14)$$

where

$$x = 2\pi\beta P_0 R_0 f_0 / \rho c^3 \quad (2-15)$$

In decibel form, the parametric gain, PG, is defined

$$PG = 20 \log |g| \quad (2-16)$$

and has been evaluated and plotted on a series of design curves.

The parametric gain, PG, is a function of three dimensionless parameters:

- (1)  $\bar{\alpha}R_o$  . The product of the mean primary wave absorption (dB/m) and the Rayleigh length
- (2)  $f_o/f_d$  . The ratio of the difference frequency,  $f_d$ , to the mean primary frequency,  $f_o$ . It is called the "downshift ratio."
- (3)  $x$  . In lieu of  $x$  it is often more convenient to use a scaled rms primary source level,  $L_o^*$ , for each primary component where

$$L_o^* = 20 \log \frac{P_o R_o}{\sqrt{2}} + 20 \log f_o \quad (2-17)$$

(kHz) (dB re 20 $\mu$ Pa-m-kHz)

which is related to  $x$  by

$$20 \log x = L_o^*(\text{dB re } 1\mu\text{Pa-m-kHz}) - 281 \text{ in water} \quad (2-18)$$

and

$$20 \log x = L_o^*(\text{dB re } 20\mu\text{Pa-m-kHz}) - 167 \text{ in air.} \quad (2-19)$$

The design curves of Moffett and Mellen can thus be adopted for air by replacing 281 (dB re 1 $\mu$ Pa-m-kHz) with 167 (dB re 20 $\mu$ Pa-m-kHz) [15].

In using the design curves, the difference frequency source level is found by adding the parametric gain to the

actual input source level utilizing the appropriate downshift ratio, scaled input source level, and absorption parameter. The directivity gain, DG, from the curves is added to the directivity index of the primary waves,  $DI_p$ , to obtain the directivity index of the secondary wave,  $DI_d$ .

$$DI_d = DI_p + DG \quad (2-20)$$

As an example of how the curves are utilized, consider the following system. A source driven at primary frequencies 4.960kHz and 5.52kHz. We have  $f_o = \frac{4.96 + 5.52}{2} = 5.24\text{kHz}$ ,  $f_d = 0.56\text{kHz}$  and downshift ratio,  $f_o/f_d = 9.3$ . If the area of the source =  $0.26\text{m}^2$ , then the Rayleigh length,  $R_o = 4.02$ . For frequency,  $f_o$ , we have  $\alpha = 3.1 \times 10^{-2} \text{dB/m} = 3.56 \times 10^{-3} \text{np/m}$  [16] and  $\alpha R_o = 0.12\text{dB}$ . If the source level of each of the primaries is 130dB re 20 $\mu\text{Pa}$ , then

$$\begin{aligned} L_o^* &= \text{scaled primary source level} \\ &= 20 \log \frac{P_o R_o}{\sqrt{2}} + 20 \log f_o \text{ (kHz)} \\ &= 130 + 20 \log R_o + 20 \log 5.24 \\ &= 156.4 \text{ (dB re } 20\mu\text{Pa-m-kHz)}. \end{aligned}$$

Now, use of Figure 2-1 yields parametric gain,  $PG = -37.5\text{dB}$  and the predicted secondary level is

$$SL_d = 20 \log \frac{P_o}{P_{ref}} + PG$$

$$= 130 - 37.5$$

$$= 92.5 \text{ (dB re } 20\mu\text{Pa)}$$

Assuming the same directivity index for each of the primaries, from Figure 2-1,  $DG = 0$  and  $DI_d$  equals  $DI_p$ .

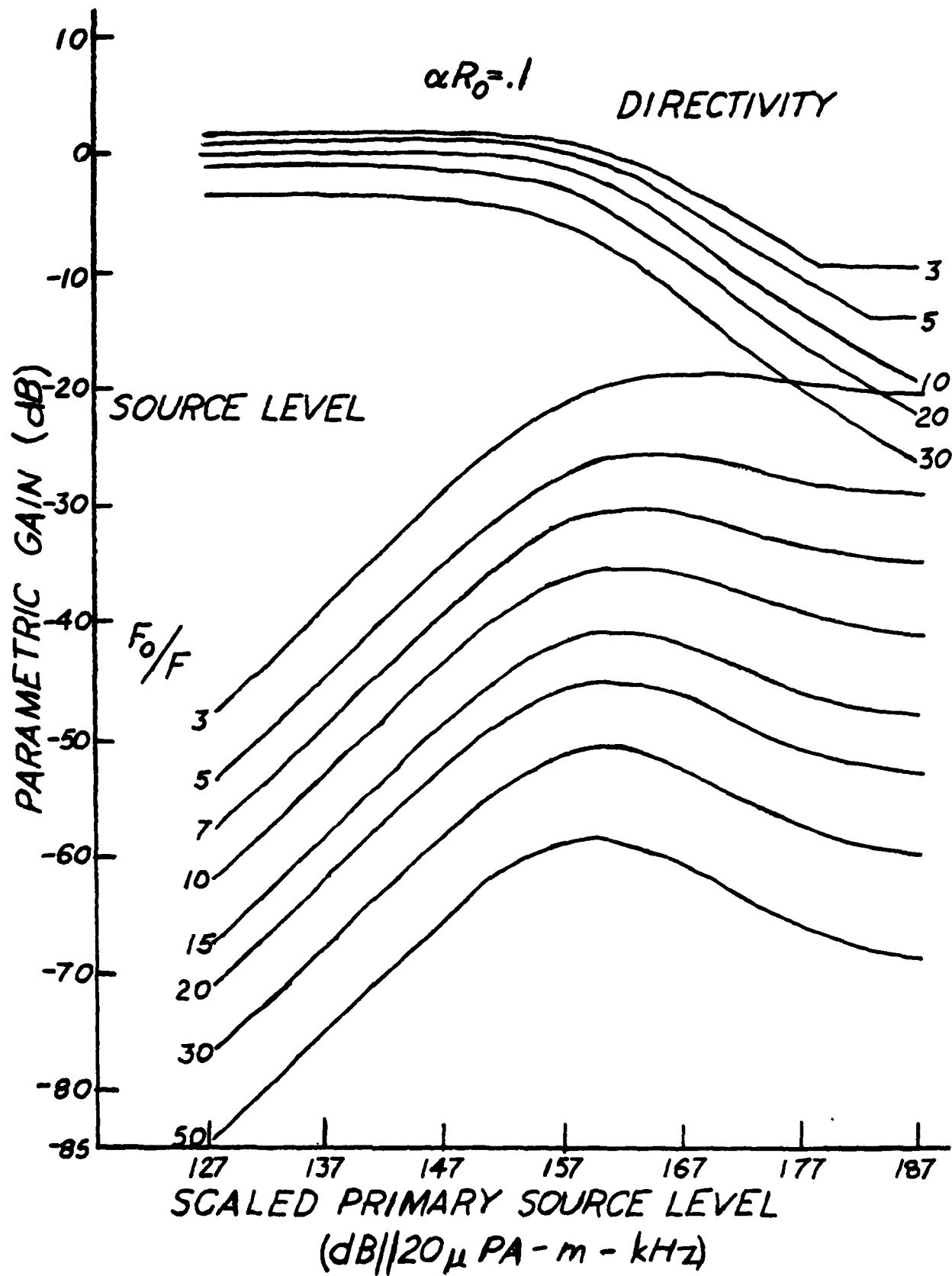


FIGURE 2-1. MOFFETT AND MELLEN DESIGN CURVE

### III. EXPERIMENTAL PARAMETRIC SOURCE

A source capable of high output over a broadband of frequencies was considered necessary to carry out a useful parametric experiment. Available at the Electroacoustics Research Laboratory, University of Texas, Austin and owned by the U.S. Coast Guard was an array, manufactured by Applied Electro Mechanics (AEM), Alexandria, Va. This AEM array had been extensively tested at the University of Texas, Austin and the basic linear parameters were reported in reference [11] and reference [12]. They are reproduced here.

#### A. ARRAY CHARACTERISTICS

The array is rectangular and composed of 20 individual exponential horns. Each horn flares exponentially from a round throat 2.5cm in diameter to a square mouth 11.4cm on a side. The horn length is 35cm and each horn is driven by a separate 35watt horn driver. The horns are bolted together to form a four element by five element array with dimensions 45.6cm by 57.5cm.

The relative frequency response of the array is shown in Figure 3-1. The array responds from 250Hz to 5800Hz with peaks at 1500Hz, 3500Hz, and 5300Hz. The beam patterns of the array at 1000Hz and 2000Hz are shown in Figure 3-2. [11] At 2000Hz, the array has become very directional with very little backward radiation. Unbaffled it very nearly meets the performance requirements of 30dB attenuation in the dark

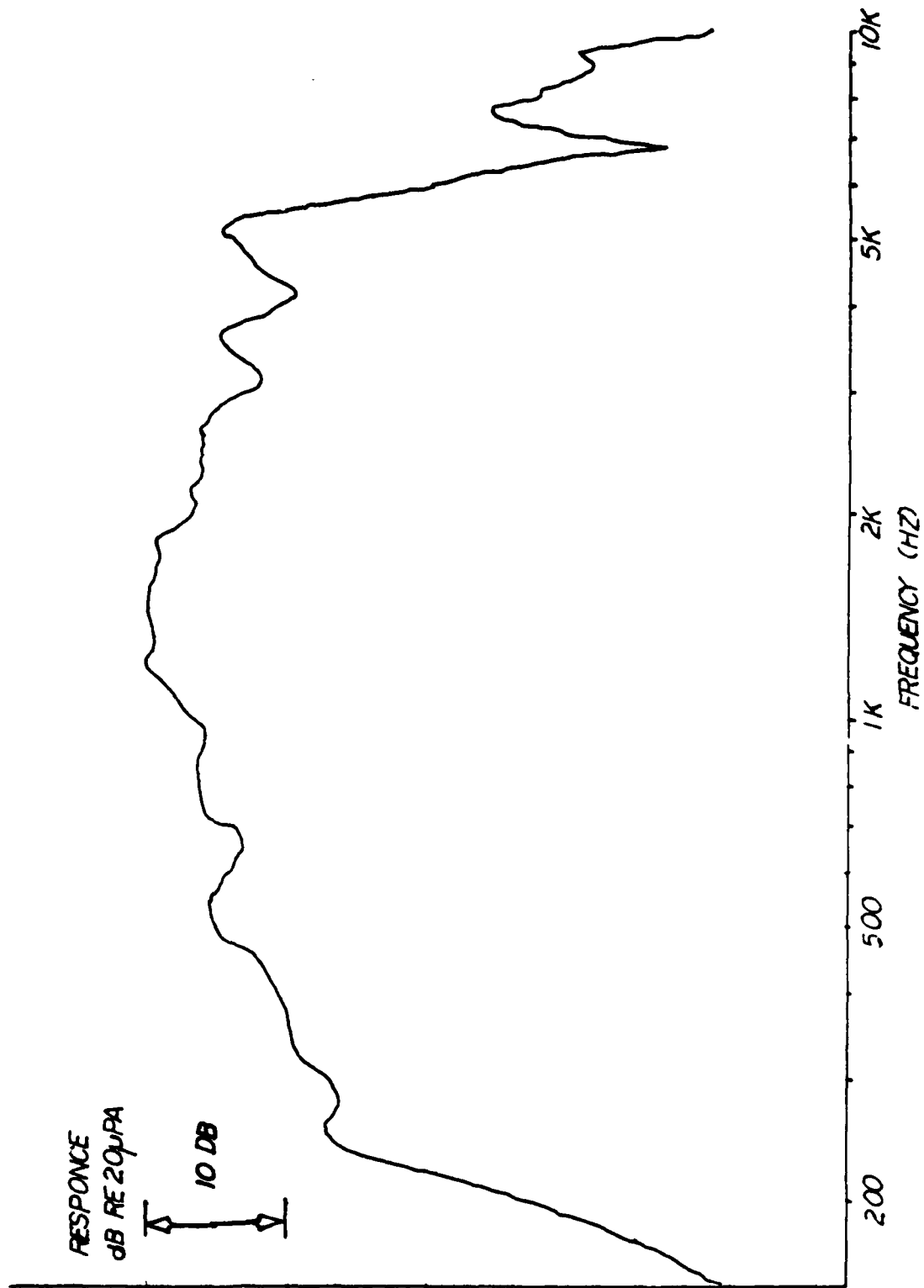


FIGURE 3-1. RELATIVE FREQUENCY RESPONSE OF ARRAY

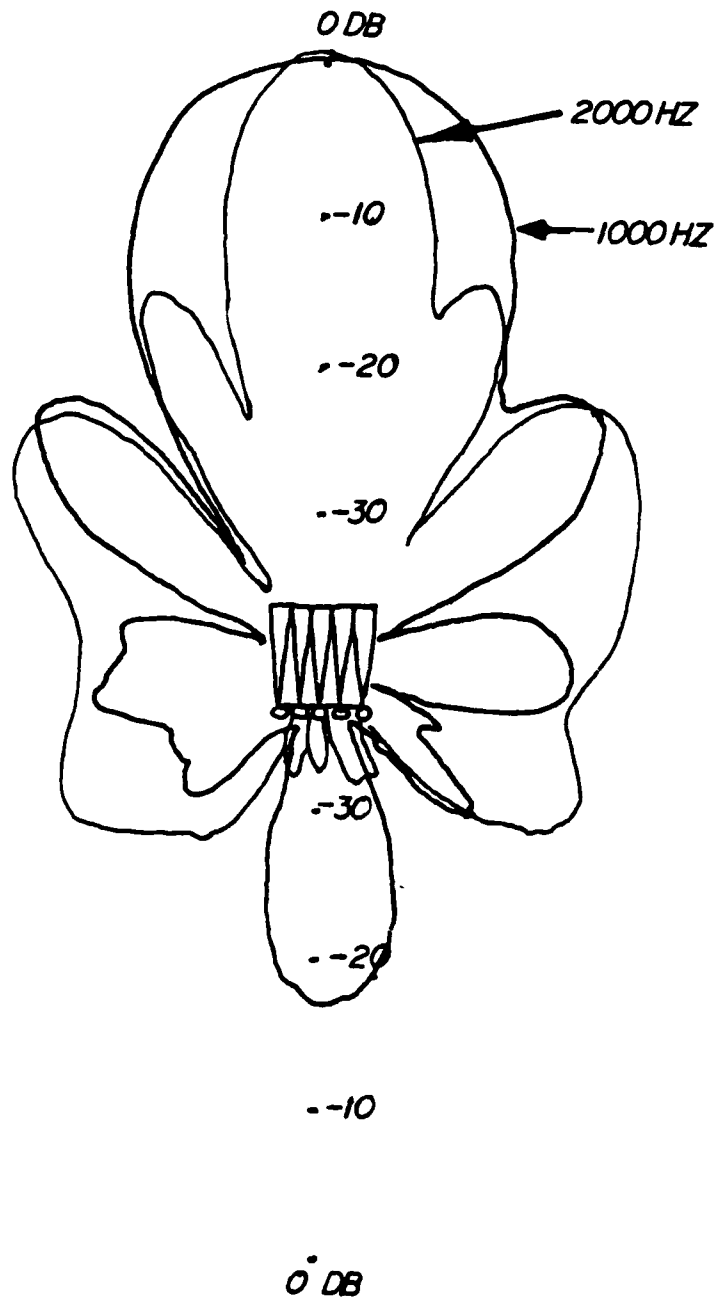


FIGURE 3-2. 1000Hz AND 2000Hz BEAM PATTERNS OF THE ARRAY

sector. A similar lack of backward radiation can be expected at frequencies higher than 2000Hz. Figures 3-3, 3-4, and 3-5 are the main lobe beam patterns across the 4 element side at the frequencies of 4240Hz, 4960Hz, and 5520Hz. These frequencies will be used to generate the parametric beam. All three beam patterns are symmetric with -3dB beam widths within experimental error of theoretical predictions.

Reference 12 reported that the array was capable of producing sound pressure levels at one meter of 146dB re  $20\mu\text{P}_a$  at 1500Hz, 144dB re  $20\mu\text{P}_a$  at 3500Hz, and 142.5dB re  $20\mu\text{P}_a$  at 5333Hz. These sound pressure levels were produced from an input of approximately 600watts. The high source levels, broadband response, and reduced backward radiation above 1000Hz made the array an attractive model parametric source.

## B. PARAMETRIC OPERATION OF THE ARRAY

The array was employed in two different ways to get an acceptable region of interaction for parametric generation of sound.

### 1. Mixed Method

Both frequencies were radiated from all twenty drivers of the array. By setting each oscillator at a primary frequency and using a resistance bridge to mix the signals, a combined signal was produced. The signal was high passed through a filter to keep only the primaries, then amplified, and sent to the array (Fig. 3-6). Care had to be taken to

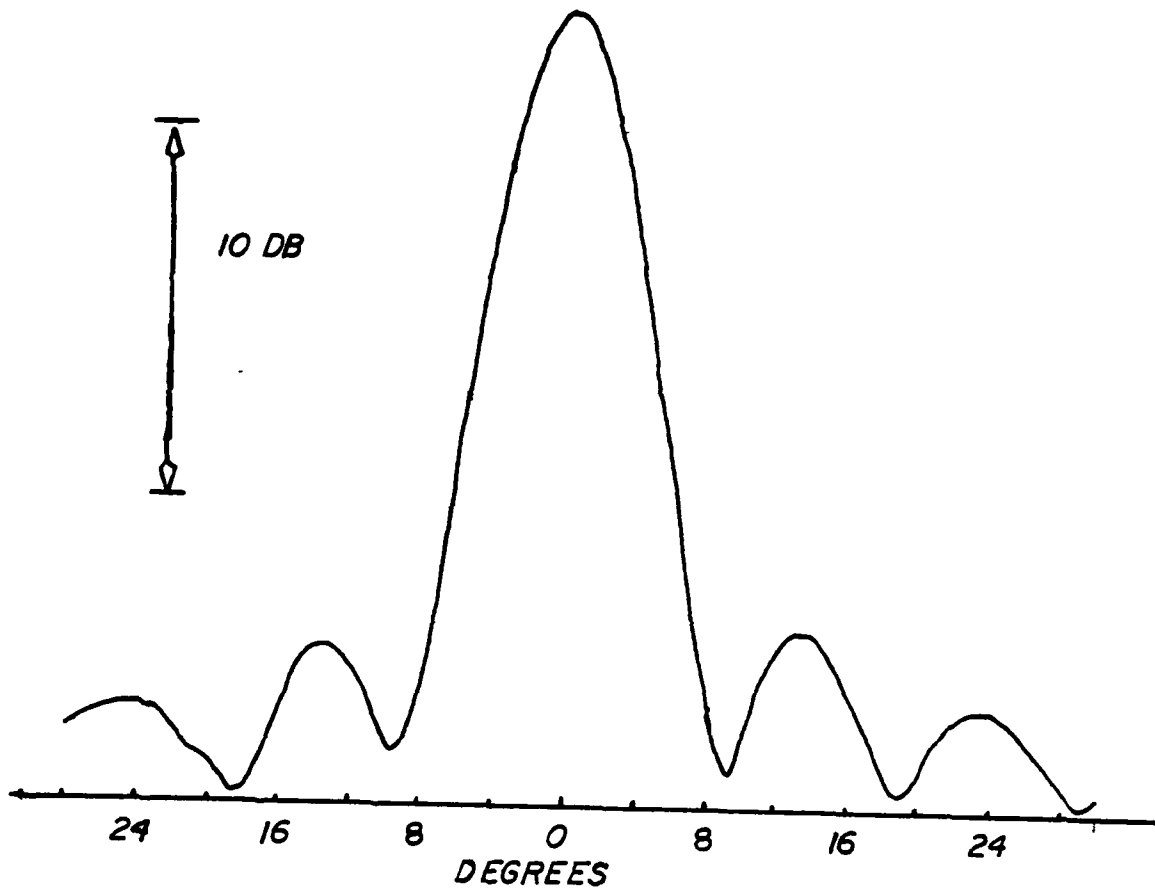


FIGURE 3-3. 4240Hz PRIMARY BEAM PATTERN

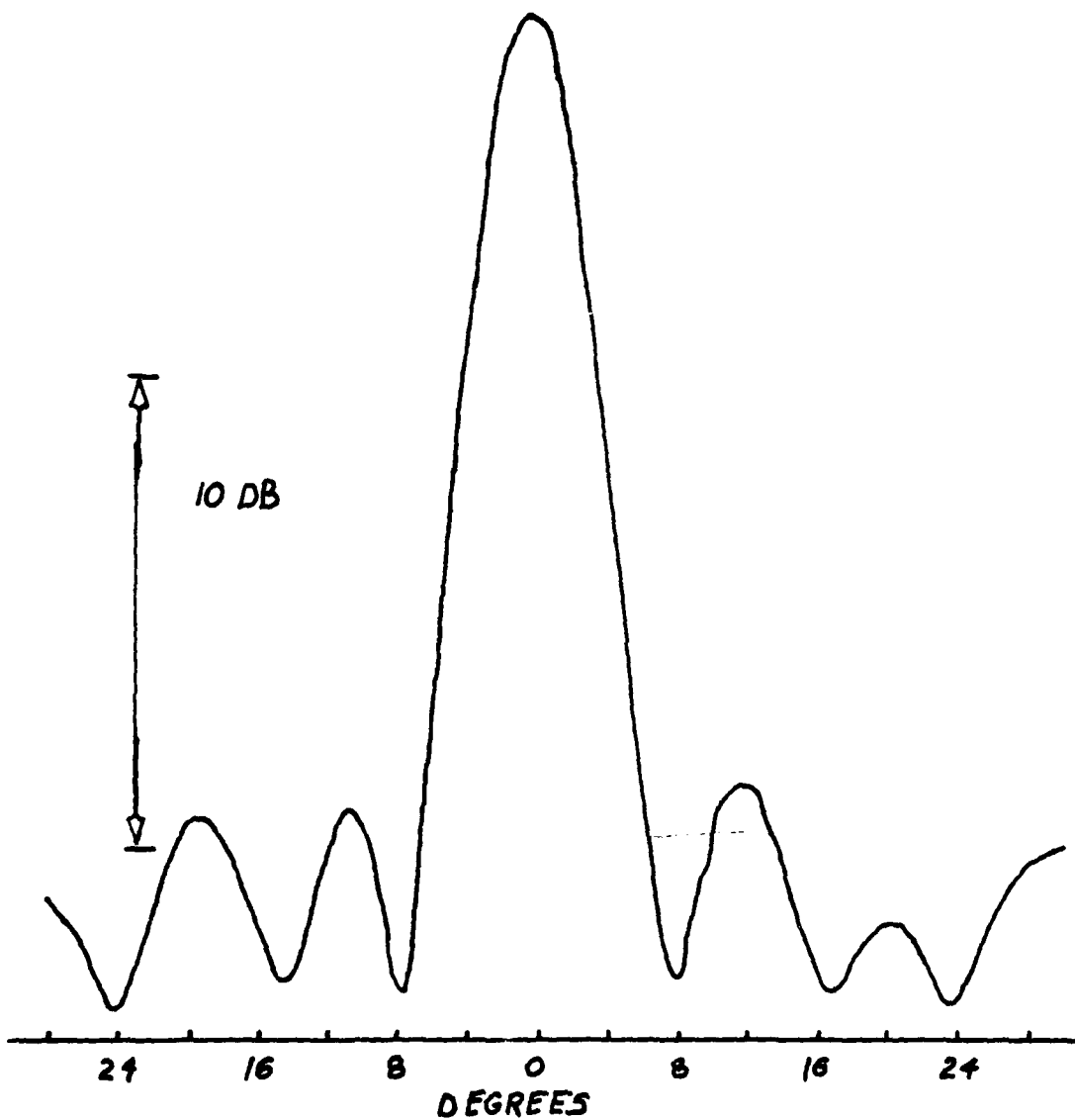


FIGURE 3-4. 4960Hz PRIMARY BEAM PATTERN

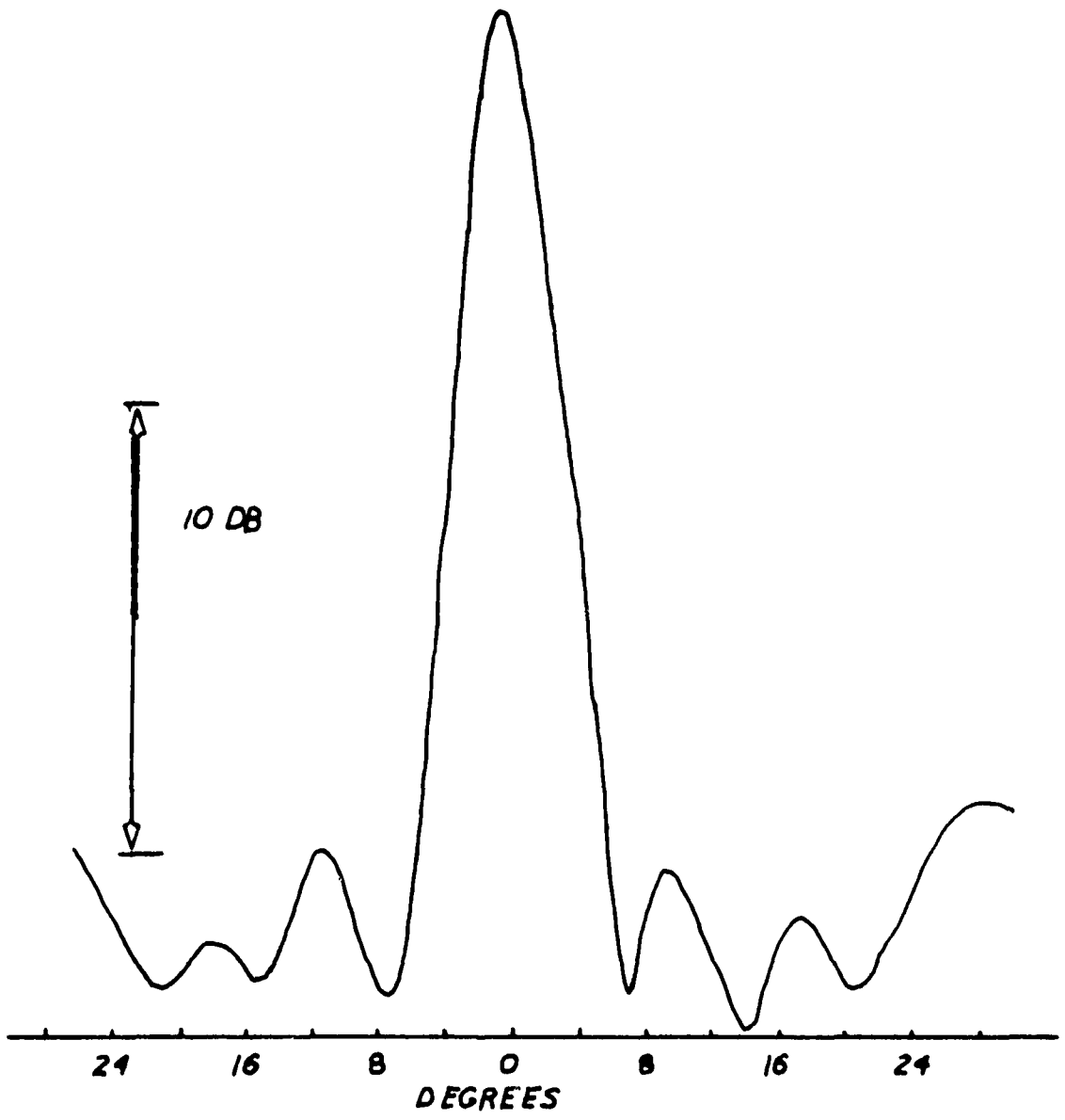
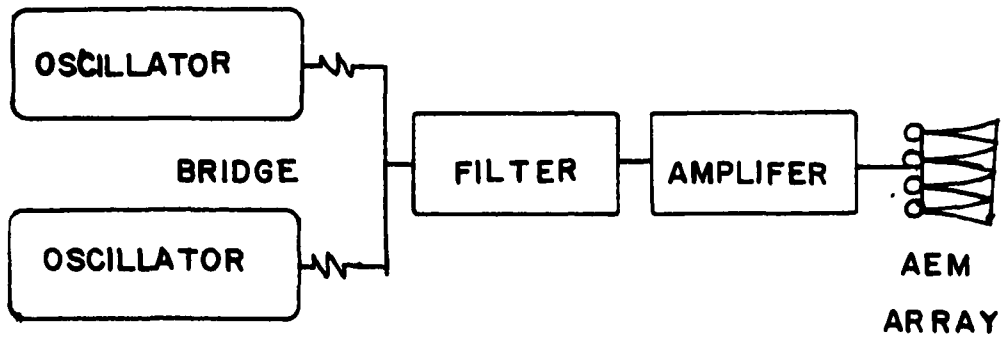
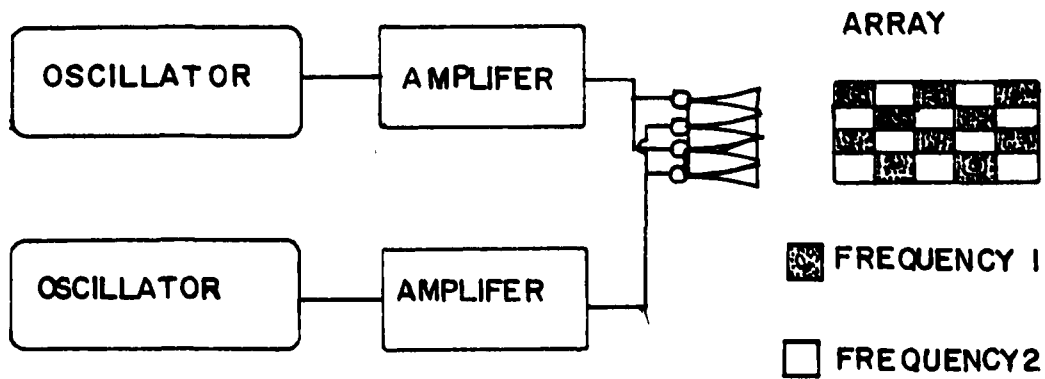


FIGURE 3-5. 5520Hz PRIMARY BEAM PATTERN



MIXED METHOD



SPLIT METHOD

FIGURE 3-6. TRANSMITTING SYSTEMS

match the output impedance of the amplifier to the input impedance of the array for two reasons: (1) impedance matching maximizes the amount of power transferred, (2) it was noted that a failure to impedance match resulted in the horns directly radiating the difference frequency through intermodulation distortion.

## 2. Split Method

In this method two oscillators (each set at a primary frequency), two amplifiers, and the acoustic sources were utilized. The array functioned as two separate sources by wiring ten drivers to one amplifier and ten drivers to the other amplifier. Each source formed a checkerboard pattern on the array face. Figure 3-6. The primary waves were electronically isolated and only mixed as acoustic waves in the air.

## C. TRANSMITTING EQUIPMENT

A list of the transmitting equipment utilized is given below:

- |                     |   |
|---------------------|---|
| (1) Oscillators     | 2 ea. GR type 1163-A decade frequency synthesizer                                   |
| (2) Filter          | Krohn-Hite Model 3202R filter   |
| (3) Power Amplifier | Kilowatt amplifier model LDV2-3 watt with selectable matching load resistances      |
| (4) Power Amplifier | Kilowatt amplifier model LDC3-2 520 watt with selectable matching load resistances. |

The kilowatt amplifiers had several capabilities which were especially useful for these experiments. For an input of 1Volt RMS they will produce full rated power output, eliminating any preamps which could introduce distortion. A 1:100 voltage divider across the output terminals of the amplifier is brought to a BNC voltage monitor connector on the front face of the amplifier. The voltage from the monitor is low enough to be spectrum analyzed to test output signal purity. The array was wired for testing as two circuits of ten drivers each. All ten drivers in each circuit were in series to raise the impedance of the network to match the output impedance of the amplifier. By wiring the drivers in series the failure of any driver would break the circuit giving an easily detectable warning of degraded array performance.

#### IV. RECEPTION AND RECEIVING EQUIPMENT

##### A. RECEPTION OF PARAMETRIC SIGNALS

In receiving parametric signals it is necessary to insure that extraneous difference frequency signals do not interfere with the actual parametrically generated difference frequency signal. Bennett identified three possible sources of extraneous signals and their properties [4]. They are:

(1) Intermodulation distortion in the receiving equipment. This extraneous signal varies as the product of the local primary amplitudes at the microphone and exhibits a propagation curve whose slope is 12dB per doubling of range.

(2) Pseudo sound interaction. This is a signal produced on the face of the receiver by radiation pressure. It also exhibits a slope of 12dB per doubling of range.

(3) Transmission distortion. This signal can be identified by its broad beam directionality. By utilizing the split transmitting method this source of extraneous signal is eliminated.

The behavior of the spurious signals is contrasted with the parametrically generated difference frequency whose propagation curve first rises with distance, reaches a broad maximum, and then gradually decreases approaching a slope of 6dB per doubling of range as the farfield of the array is reached [4].

## B. RECEIVING EQUIPMENT

Three different receiving systems were tested. The goal was to find the system that minimized the extraneous difference frequency signals. Characteristics of the three systems tested are listed below.

Receiver	1/2" ALTEC BR-150 Microphone	1/2" ALTEC BR-200 Microphone	LC-10 Hydrophone
Sensing type	Condenser	Condenser	Lead Zirconate Titanate
Sensitivity re 1 volt/ μbar	-58dB	-85dB	-108dB
Linear Limit	158dB	185dB	-
Average Noise Threshold SPL re 20μPa	58dB	85dB	-
Frequency Response	10Hz - 6500Hz	30Hz- 6000Hz	.1Hz to 120kHz
Power Supply	ALTEC 526B	ALTEC 526B	none
Amplifier	none	none	HP465A with 40dB amplification

Each receiving system was configured identically to its proposed method of operation during actual parametric testing. For the ALTEC BR-150 and BR-200 the system included the microphone, power supply and 150' of microphone cable. The LC-10 system included the hydrophone, amplifier and 150' of cable.

To measure the intermodulation of the microphone systems the array was configured in the split transmitting method. This eliminated the chance of any transmitted spurious difference frequency signal. Each microphone was placed less than 0.5m from the array. The array was turned on, and the levels of the primaries received by the microphones were varied. As the microphones were very close to the source it was assumed that any difference frequency being recorded was the result of intermodulation in the receiving system and not parametrically generated. This was a safe assumption as the overlap distance of the two adjacent units in the split system was .41m. The spurious difference frequency generation in the receiving equipment and pseudo-sound could be measured in total. The results are plotted as equivalent sound pressure level of the spurious signal vs. sound pressure level of the primary signals at the microphone. Fig. 4-1. Also noted is the noise threshold of each system.

The LC-10 hydrophone was chosen as the receiving system. For a given primary input it had 30dB less intermodulation than the BR-150 and 5dB less than the BR-200. The LC-10 observed noise threshold was 13dB less than the BR-150 and 40dB less than the BR-200. A primary signal to difference frequency intermodulation ratio of 60dB established the lower limit of the level of parametric signals which could be measured by the LC-10.

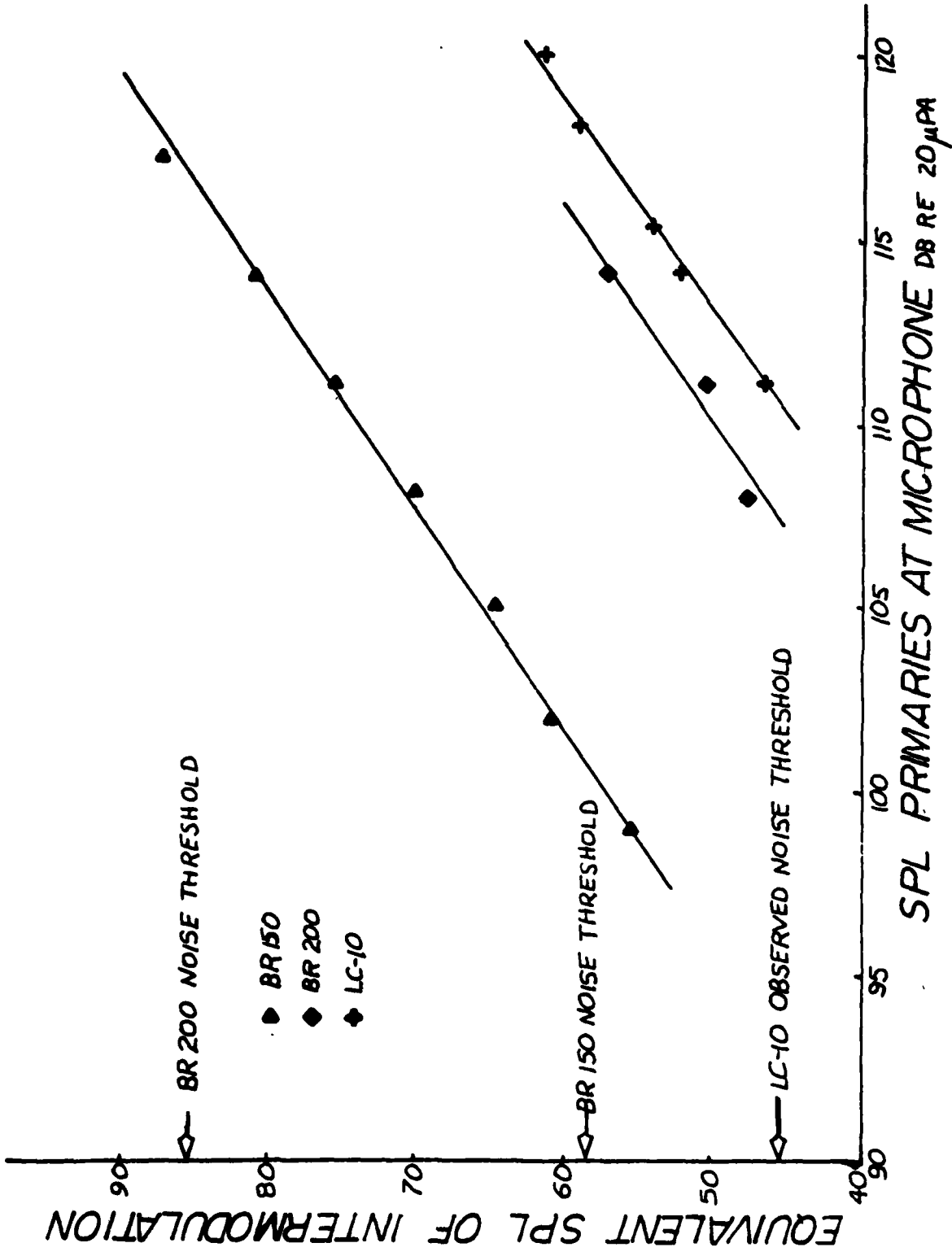


FIGURE 4-1. INTERMODULATION IN RECEIVING SYSTEMS

The remainder of the receiving equipment included:

- |     |                           |                            |
|-----|---------------------------|----------------------------|
| (1) | Spectrum analyzer         | Schlumberger Model 1510-03 |
| (2) | Wave analyzer             | HP Model 302A              |
| (3) | Filter                    | Krohn Hite Model 3202R     |
| (4) | Sound level<br>calibrator | GR Type 1562-A             |

The Schlumberger Model 1500-03 was utilized as the level recording device. The model 1510-03 is a fully-digitalized instrument that provides real time spectral analysis of analog signals. It has five full scale input ranges from 0.1V full scale to 10V full scale. The input signal to the model 1510-03 is divided into 256 spectral bands (lines of resolution) across one of 10 selectable frequency bands of interest. The frequency spacing of the lines of resolution vary from 0.1Hz to 100Hz. For one testing on the primary frequencies (5000Hz) a 40Hz spectral bandwidth with a 12.8s averaging time was used. For the difference components, at 1280Hz, a 10Hz spectral bandwidth with 6.4s averaging time and, at 560Hz, a 4Hz spectral bandwidth with 16s averaging time were utilized. To measure the correct levels care was taken to choose frequencies that placed the primary and secondary frequencies in the center of the rectangular sampling window of the spectrum analyzer. The difference frequencies were also chosen to coincide with spectral bands that had low noise levels.

### C. DATA ACQUISITION

The initial testing of the array at the Naval Postgraduate School was done in the anechoic chamber. The maximum distance that a signal could be propagated in the chamber was 7m. The farfield of the array is generally considered to begin at  $1/2\alpha_0$  where  $\alpha_0$  = average primary absorption in np/m. For a 5000Hz signal the distance to the farfield is approximately 125m. The 7m propagation distance was considered to be too short to get useful data so the experiment was moved outdoors. The outdoor experiments were done using the Mars Radio Tower on the grounds of the Naval Postgraduate School. The array was placed facing upward 2.5m from the tower on a level stand. The stand was leveled prior to each data run with a carpenter's level placed on the face of the array. The level was measured to be accurate to within  $1/4^\circ$ . The receiving microphone was attached to a boom and extended 2.5m out from the tower. A system of two surveying theodolites was used to position the microphone directly over the center of the array. The positional accuracy of the microphone was within 2cm of the acoustic axis of the array.

The propagation distance was varied by moving the boom to different heights on the tower. There were only four possible propagation distances the maximum of which was 30m. Scattering from the tower was ignored as the dimensions of the tower stock were much less than the wavelengths of the primaries.

To take beam patterns outdoors the array was placed on a tiltable platform. It was leveled using a carpenter's level. To measure angles a 12-inch protractor was taped to the side of the array with the protractor's base level with and parallel to the face of the array. A line and plumbob, attached at the apex of the protractor and calibrated to read  $0^\circ$  when the face of the array was level, were used to measure angles of tilt. The maximum angle that could be measured with this system was about  $5^\circ$ . For more complete beam patterns the array was placed in the anechoic chamber at the Naval Postgraduate School. A small motor turns the source while simultaneously sending a signal to the X-scale on the plotter. The level of the signal from a microphone mounted in the chamber is sent to the Y-scale of the plotter.

#### D. EQUIPMENT CHECKOUT AND CALIBRATION

Prior to the collection of data the following checks were made:

(1) The LC-10 hydrophone was comparison calibrated with a BR-150 microphone. The BR-150 was first calibrated with a GR-1652-A piston calibrator. The LC-10 and the BR-150 were then placed at the same position in a sound field and the responses compared.

(2) The Schlumberger spectrum analyzer was calibrated using its internal signal generator.

(3) The array was precisely positioned using the theodelites and the carpenter's level.

(4) The array was checked for driver failure by simply sending a signal through each circuit and listening for a response.

## V. EXPERIMENTAL INVESTIGATION

Initially, the purpose of this investigation was to test the array in a fog signaling configuration where the primaries would be set around 2000Hz and the difference frequency would be around 400Hz. This configuration had to be abandoned as the testing generated noise complaints from the occupants of residential areas near the testing tower. In order to continue testing without causing more noise complaints, the primary frequencies were raised to the vicinity of 5000Hz. The noise complaints stopped after this step was taken.

It was concluded that this research would concentrate on the verification of the ability of the Moffett and Mellen design curves to predict the source level of the difference frequency in air. Only the single data point from Brinkman's experiment was previously available to compare with the Moffett and Mellen predictions.

### A. PROPAGATION

The Moffett and Mellen design curves are farfield predictions for the parametric array. Based on a 5000Hz primary frequency, a farfield distance of 130m was expected for the experiment. As the maximum range of observation was 30m, all measurements were limited to the nearfield of the parametric array. Theoretically, the difference frequency

propagation curve in the nearfield should first rise with distance, reach a broad maximum and then decrease approaching a slope of 6dB per doubling of range as the farfield of the array is reached. Mellen [13] and Rolleigh [14] have developed correction factors for the nearfield. Plotted in Figures 5-1 and 5-2 are the extrapolated farfield spreading curves as predicted by Moffett and Mellen. Below this curve is the Rolleigh nearfield propagation curve. Rolleigh's result is limited to the spherical spreading region of the primaries, which is greater than 4m in both cases. Mellen's prediction, although not plotted, gives a similar curve.

The data plotted in Figures 5-1 and 5-2 are observed from the split transmitting method. At short range the data appear below the predicted level but at longer ranges they approach the Rolleigh prediction. This behavior is probably the result of the split transmitting method. The beam width of each individual horn is  $33^\circ$  at 5000Hz. Not until the sound has propagated approximately 2.0m do the beams of all units overlap. This would indicate that the first 2.0m of the interaction region is somewhat weakened. This loss of interaction region is not important at longer ranges because this is a farfield source where the bulk of the interaction takes place in the farfield of the primary waves. The loss of the first of the interaction region in the nearfield could be responsible for the low readings at short ranges.

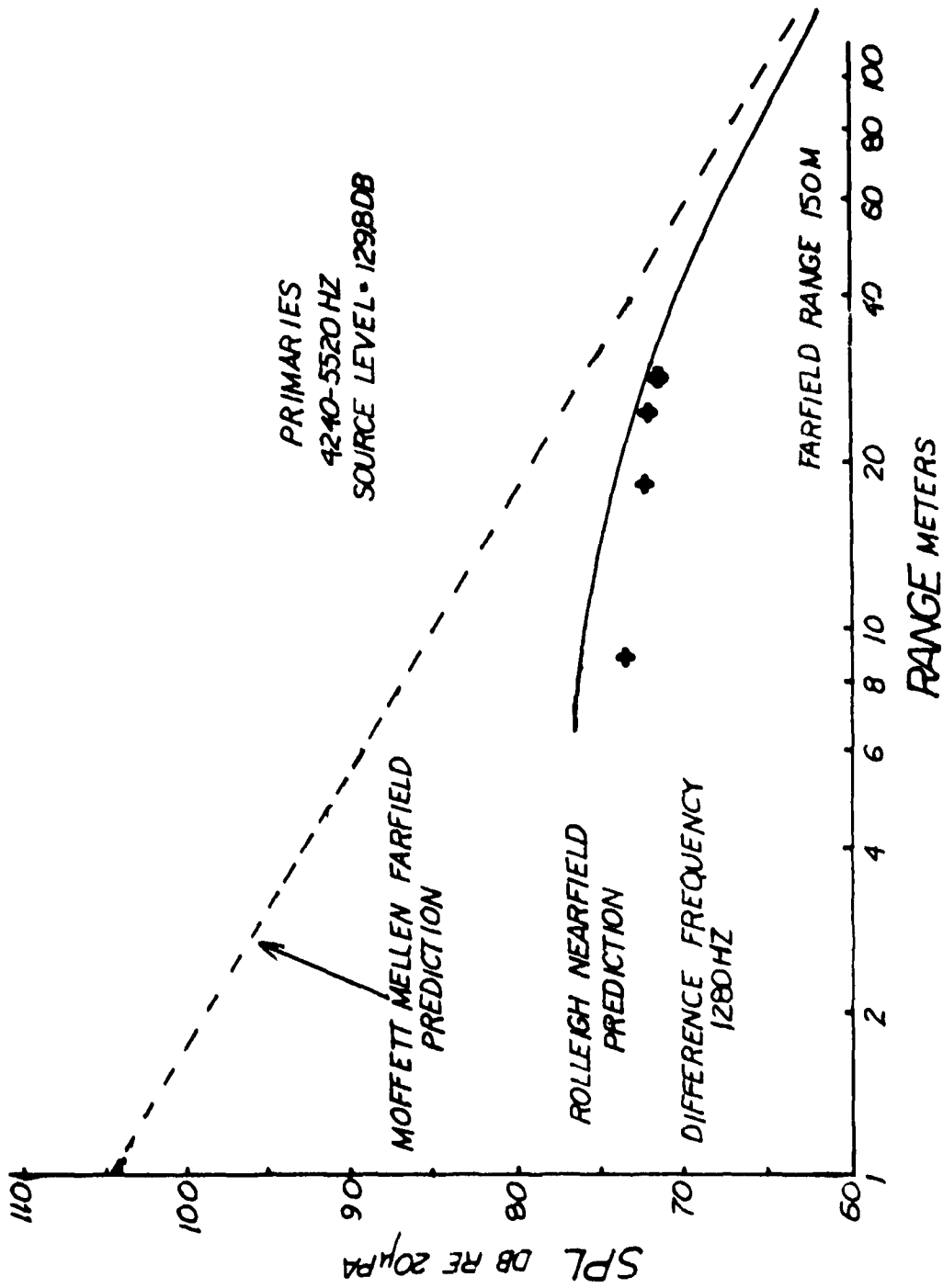


FIGURE 5-1. PROPAGATION CURVE OF 1280HZ DIFFERENCE FREQUENCY BEAM

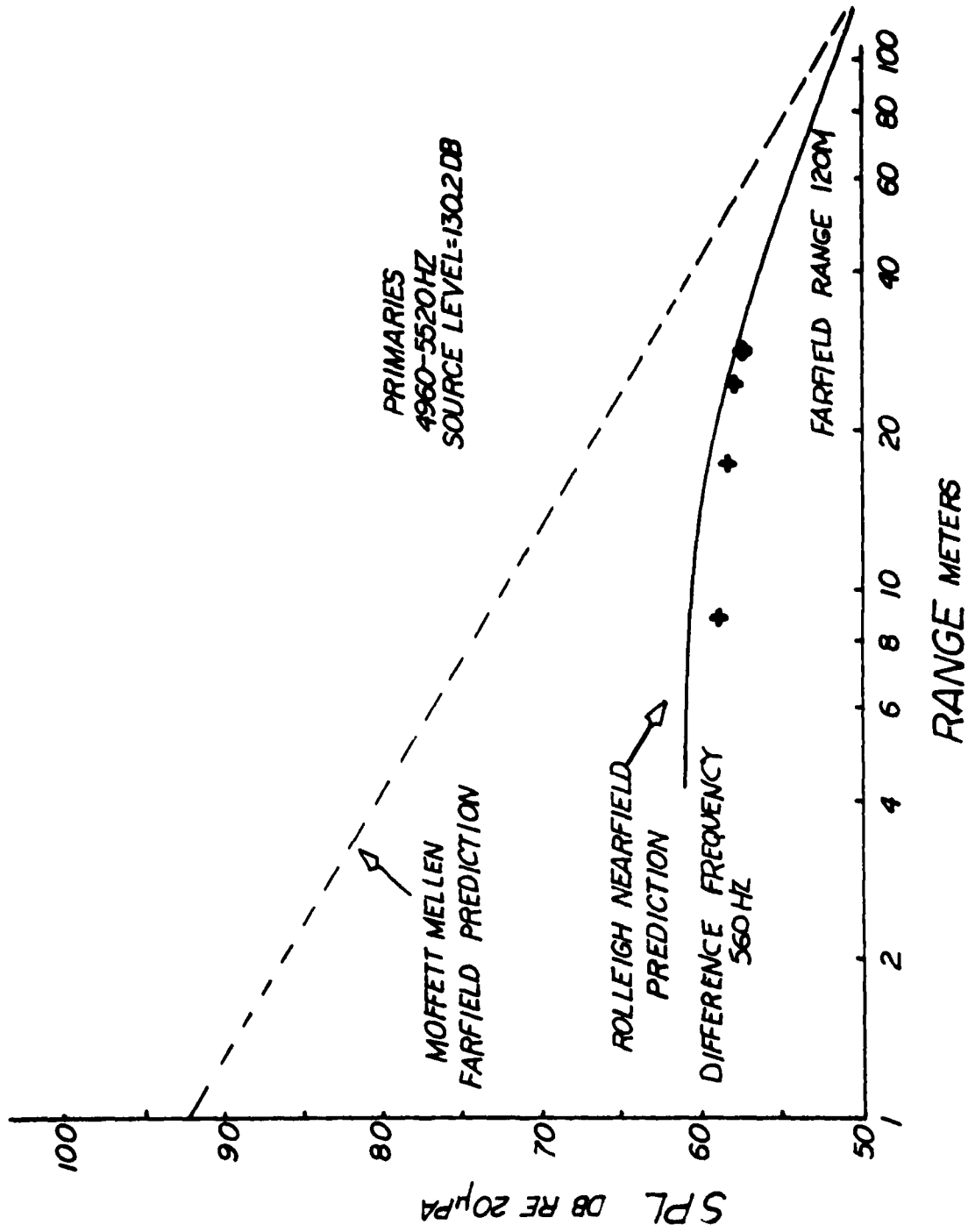


FIGURE 5-2. PROPAGATION CURVE OF 560HZ DIFFERENCE FREQUENCY BEAM

## B. SOURCE LEVEL DIFFERENCE VS. SOURCE LEVEL PRIMARY

In reviewing the Moffett and Mellen design curves it can be noted that at low primary source levels a 3dB increase in the primaries source level produces a 3dB increase in the parametric gain or a 6dB increase in the secondary source level. This behavior is predicted by Westervelt, and Berklay and Leahy, for an absorption limited parametric array (where the level of the secondary varies as the product of the primary levels).

At high levels of 3dB increase in the primaries produces less than a 6dB increase in the secondary. This is the saturation region of the array. In this region energy instead of being coupled into the difference frequency, as is done at low levels, is being lost in the generation of harmonics of the primaries.

The array had enough flexibility in source level to compare to the saturation effects with the predictions of Moffett and Mellen. To observe this behavior the microphone was placed on the propagation axis at 27.5m and the output of the primaries varied from low to high levels. The Moffett and Mellen source level predictions are for the farfield region while the observation point at 27.5m was in the nearfield. +4dB was added to the data points at 1280Hz and +5dB was added to the points at 560Hz. These are the corrections predicted by Rolleigh for the nearfield at 27.5m. With this correction and extrapolating both the difference frequency and the primaries back to one meter, it is possible

to make a plot of source level difference frequency versus source level of one primary. See Figures 5-3 and 5-4. Illustrated on the graph are the Moffett and Mellen predictions and a prediction for the level in a strictly absorption limited case.

To verify that saturation is taking place pictures were taken of the spectrum at 6.5m for low primary source level of 122dB re 20 $\mu$ Pa and high primary source level of 130dB re 20 $\mu$ Pa. The top photograph in Figure 5-5 is the spectrum recorded at 6.5m from the low primary source level, the bottom photograph is the spectrum from the high level input. Visible to the right of the two primaries in each photograph are the second harmonics and the sum frequency. At the higher primary levels the second harmonics are 7dB closer to the first harmonic levels than at the low level, which represents a loss of energy from the interaction region.

By shortening the interaction region, saturation also broadens the difference frequency beam patterns. Figure 5-5 illustrates the amount of broadening that occurred in the difference frequency beam pattern between low level, 120dB re 20 $\mu$ Pa, and high level, 130dB re 20 $\mu$ Pa. At low levels, the difference frequency beam pattern should be the product of the primary beam patterns [10]. At high levels, the difference frequency beam pattern is broader and can be estimated from the Moffett and Mellen curves [6].

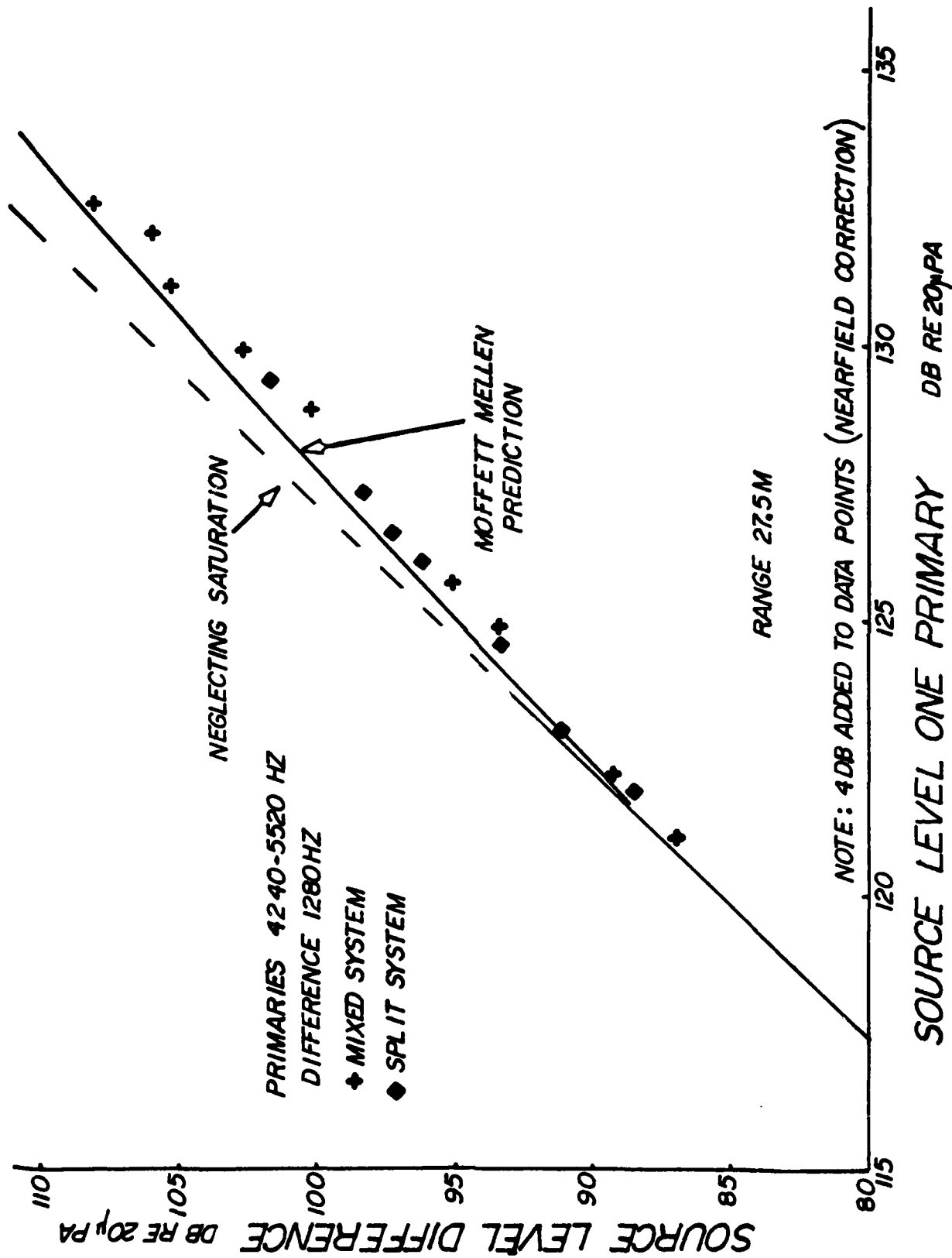
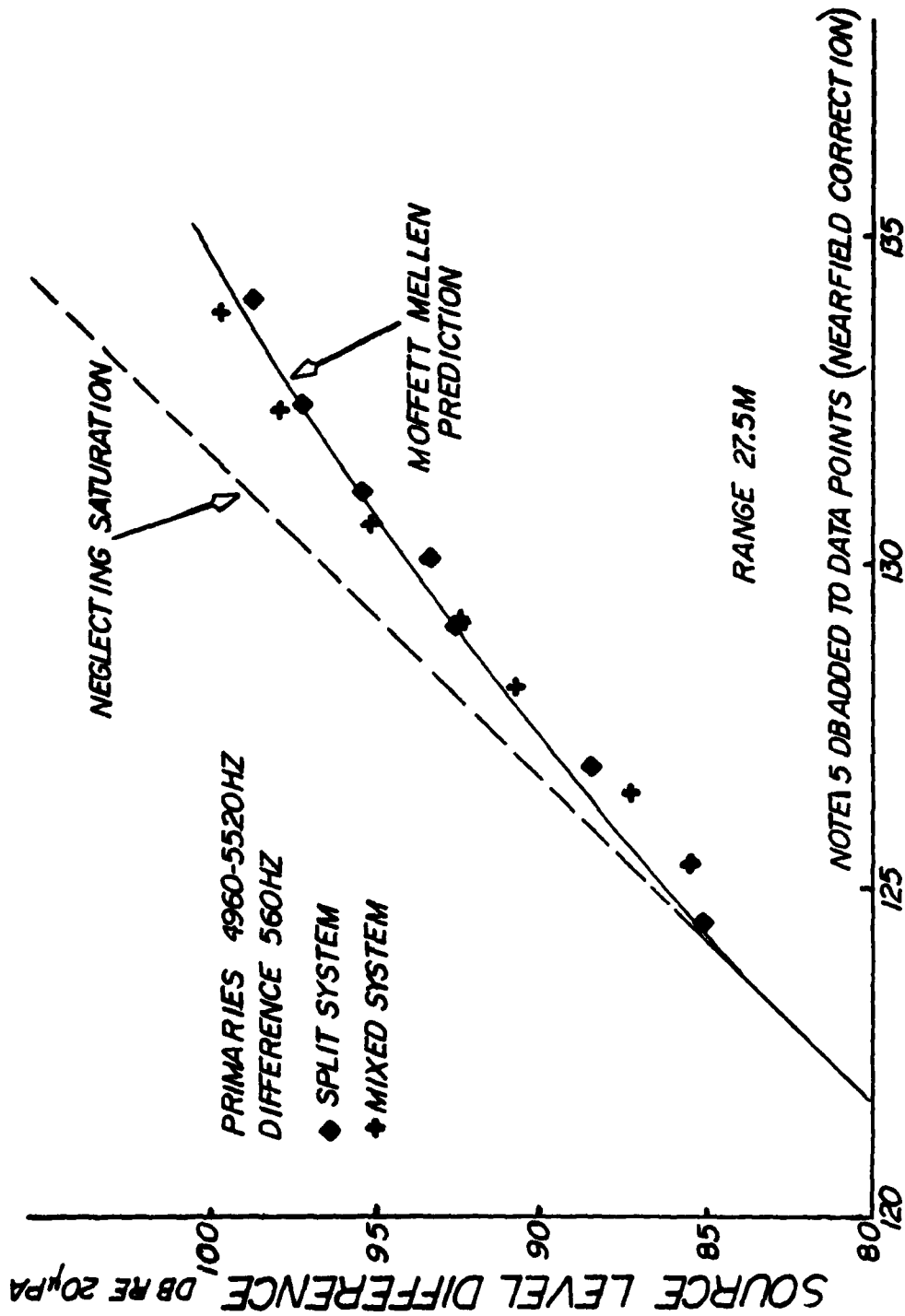


FIGURE 5-3. SOURCE LEVEL PRIMARY VS. SOURCE LEVEL 1280Hz DIFFERENCE FREQUENCY BEAM



SOURCE LEVEL ONE PRIMARY DB RE 20 $\mu$ PA

FIGURE 5-4. SOURCE LEVEL PRIMARY VS. SOURCE LEVEL 560HZ DIFFERENCE FREQUENCY BEAM

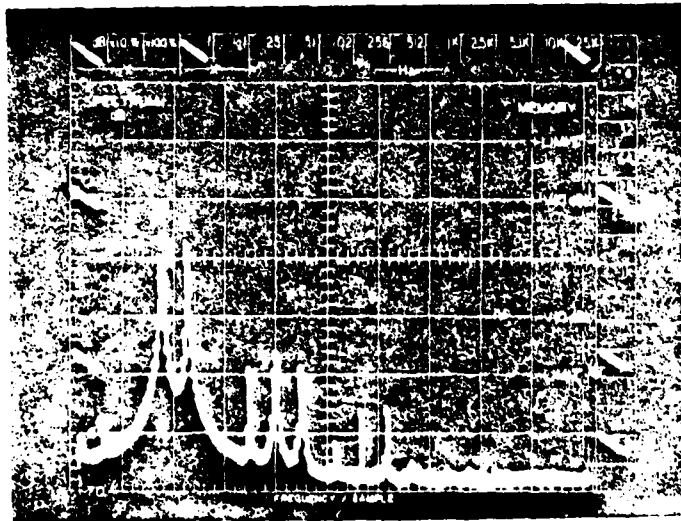
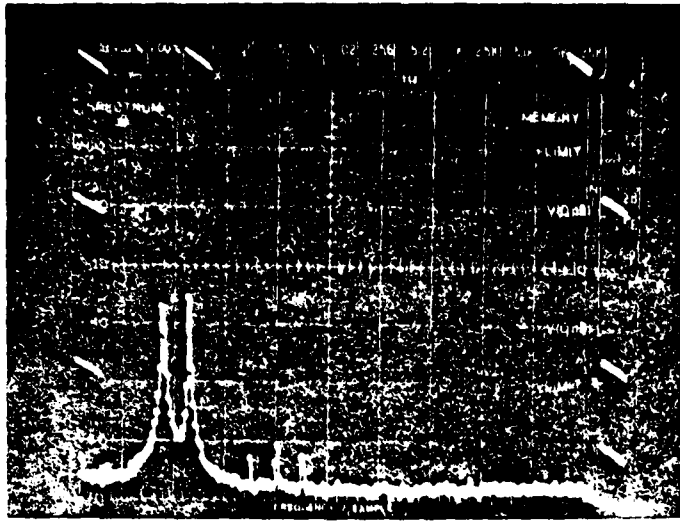


FIGURE 5-5. LOW SOURCE LEVEL AND HIGH SOURCE LEVEL SPECTRUMS AT 6.5m

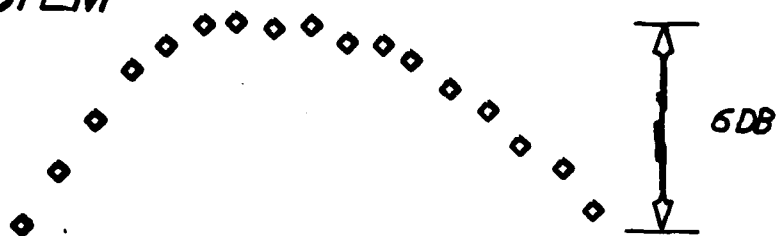
The theoretical pattern for the low level was calculated by multiplying the theoretical directivities of a 4240Hz beam and a 5520Hz beam calculated from the dimensions of the 5 unit side of the array. The theoretical pattern for the high level was found assuming 0dB directivity gain from the design curves and adding it to an average directivity of the two primaries. Both predictions are consistent with the data. Figure 5-7 is a wider view of the 1280Hz difference frequency beam taken at 6.5m which illustrates the narrow, sidelobe-free beam shape of the difference frequency.

#### C. SPLIT AND MIXED TRANSMITTING

One concern of this experiment was determining the equivalency of the split and mixed transmitting systems. Two experiments had failed to get an acceptable region of interaction from a horn driver system in air configured as a split transmitting system [3], [4]. As noted in the previous section, it appeared that the first 2m of the interaction region was being lost with the split system. This loss was found not to be significant when the source level primary versus source level secondary data runs were made again with the array in a mixed transmitting system (Figures 5-3, 5-4). In comparing the two systems, no trend is evident in the data to suggest an effect from split transmitting when the data are taken at 27.5m.

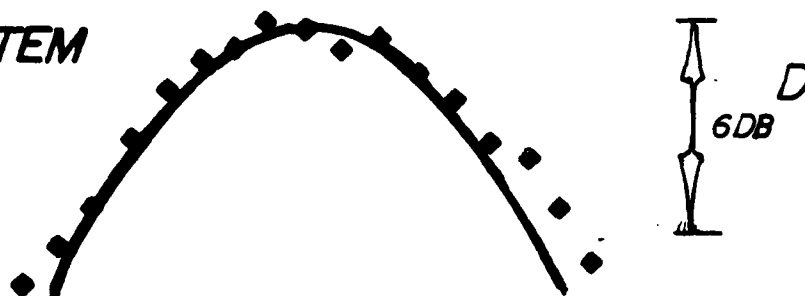
### MIXED SYSTEM

◆ LOW LEVEL  
0 DB = 57.5 DB



### SPLIT SYSTEM

◆ LOW LEVEL  
0 DB = 53.5 DB



▲ HIGH LEVEL  
0 DB = 69.2 DB

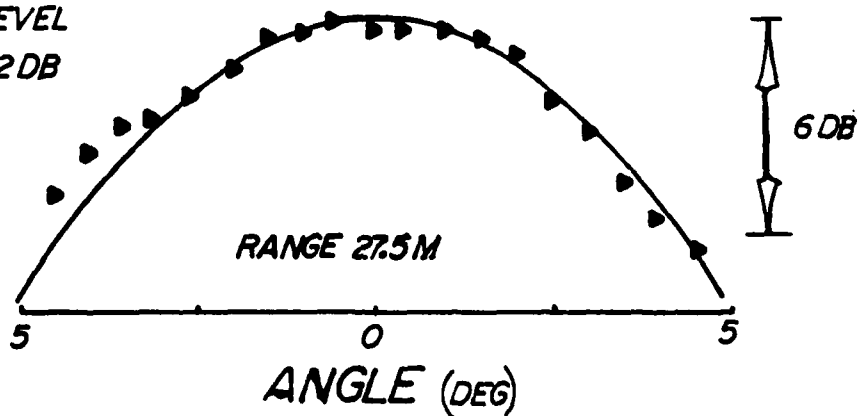


FIGURE 5.6. 1280Hz DIFFERENCE FREQUENCY BEAM at 27.5m

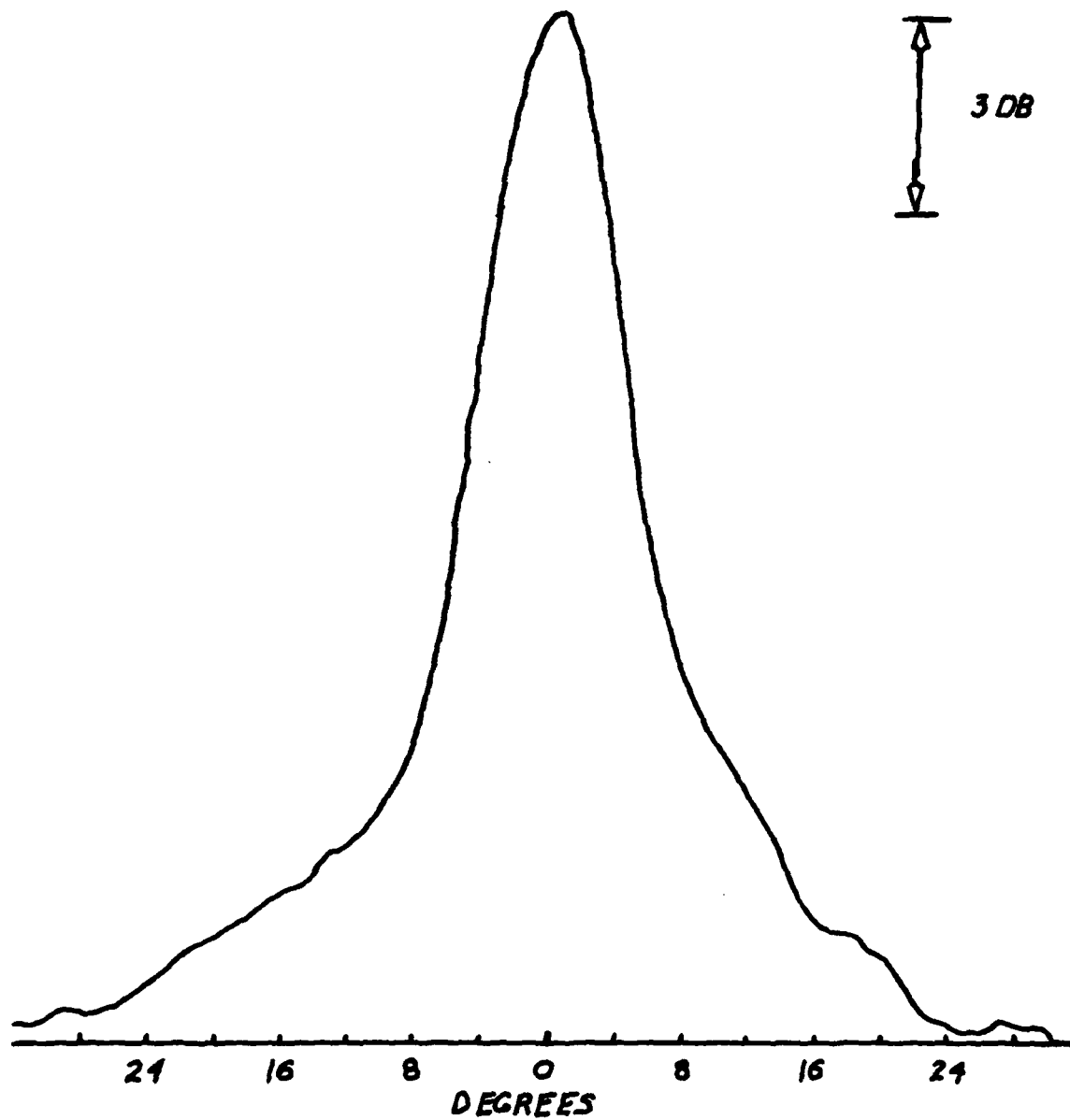


FIGURE 5-7. 1280Hz DIFFERENCE FREQUENCY BEAM AT 6.5m

## VI. RESULTS AND CONCLUSIONS

### A. EXPERIMENTAL PROPERTIES AND THEORETICAL PREDICTIONS

This experimental work on the parametric array in air was able to demonstrate several properties of the array that had not been verified before:

(1) An acceptable region of interaction from two electrically isolated sources of horn drivers generated a difference frequency which behaved almost identically to an equivalent mixed electronic system (Figs. 5-3, 5-4).

(2) The slope change in the source level curves of Moffett and Mellen was observed when the source began to saturate. By applying the nearfield correction of Rolfeigh, excellent agreement was shown between the Moffett and Mellen predicted levels and the experimental data (Figs. 5-3, 5-4).

(3) The behavior of the parametric array in the nearfield was found to follow the nearfield predictions of Rolfeigh. At the shortest ranges the data are below the predicted level. This is probably the result of using the mixed transmitting system where the interaction region at distances of less than 2m are lost. This loss does not affect the overall behavior of the array as the bulk of the interaction takes place at a distance greater than 4m, but could effect the propagation curve in that region of the nearfield close to the source (Figs. 5-1, 5-2).

(4) Difference frequency beam broadening was observed as the array length became limited by saturation (Fig. 5-5).

#### B. FOG SIGNALING CAPABILITY

Although it was not possible to test the array in an optimal fog signaling configuration the Moffett, Mellen design curves make it possible to propose a field configuration for a parametric fog horn.

The proposed horn would be a 50-unit array, area  $0.5\text{m}^2$ , operating with primaries around 2000Hz and secondary around 500Hz, input power 1200 watts, and source level primaries of 145dB. Entering the design curves:

Primary = 2kHz      Secondary = 500Hz      Downshift = 4

$$\alpha_{2000} = 0.009\text{dB/m} \quad R_c = \frac{.5\text{m} \cdot 2000}{340} = 2.9\text{m}$$

$$\alpha R_o = 0.02\text{dB}$$

$$\begin{aligned} \text{Scaled Source Level} &= 145 + 20 \log 2.9 + 20 \log 2 \\ &= 160\text{dB re } 20\mu\text{Pa-m-kHz} \end{aligned}$$

From Fig. 2-1 , parametric gain = -20dB

Difference Frequency Source Level = 125dB re 20 $\mu$ Pa.

This proposed parametric fog horn will be compared with a linear horn operating at 500Hz. In general, the amount of

unwanted sound in the dark sector of the fog signal will depend on several factors. These include source directionality, baffle attenuation, atmospheric absorption, geometric spreading, physio acoustic effects of the ear receiver and psycho acoustic perception.

The difference frequency beam is narrow, nearly side-lobe free. Any noise from the parametric fog horn will be from the primaries at 2000Hz, while noise from the linear source will be at 500Hz. To get the same source level at 500Hz the parametric primaries will have to be 20dB higher than the linear signal. At the face of the array the parametric fog horn will be 20dB higher in level.

The directionality of the array reduces the parametric signal behind the array. The array is nearly omnidirectional at 500Hz but at 2000Hz it is 30dB down in the backward direction.

Both sources could be baffled to further reduce backward radiation. The parametric signal due to its shorter wavelength would require a smaller baffle than the linear signal for similar attenuation.

Both signals would spread geometrically at the same rate, but the parametric signal would be attenuated faster due to its greater atmospheric absorption. The atmosphere absorbs 500Hz at 26dB/mile and 2000Hz at the rate of 15.9dB/mile.

The physioacoustic and psychoacoustic effects are the most difficult to predict. It is known that the human ear

is more sensitive at 2000Hz than at 500Hz giving a perceived sound level gain to the parametric signal. Conversely the parametric signal, which is made up of two frequency components, with proper frequency selection could present a much more pleasing pitch raising the level of tolerance of the signal above a simple pure tone of equal intensity.

The parametrically generated difference frequency beam is quite narrow compared to the angular width a fog signal normally illuminates. To compensate for the narrow beam the source would have to be scanned. This can be accomplished by mechanically moving the entire array assembly through the angles desired. Another method would be to electronically scan the signal.

In the experimental work all horn drivers were driven in phase which creates a beam pattern where the major lobe is perpendicular to the length of the array. By introducing a time delay, i.e., phase difference between the acoustic signals generated at neighboring drivers, the major lobe can be pointed in an arbitrary direction. With a micro-processor control unit the time delays could be continuously varied to steer the beam over any angle desired.

One capability from narrow beams and steering not available from the present omnidirectional fog horns is the ability to vary the signal content to different sectors. For example a signal could be programmed to transmit a short, then long blast to sectors to the left of a navigation channel, a long blast right down the channel and a long

then short blast to sectors to the right of a channel. Similarly, a shoal could have a different signal transmitted over it than the rest of the sectors, as is done with sectored lighthouses.

#### C. DISADVANTAGES OF A PARAMETRIC FOG HORN

The primary disadvantage of a parametric fog horn would be cost of acquisition and operation. The proposed fifty horn unit with associated amplifiers and oscillators could cost \$25,000 each. Parametric generation of sound is also very inefficient. To generate a 125dB re 20 $\mu$ Pa signal linearly would take less than ten watts input whereas the parametric input would be 1200 watts. Additionally, due to the need to scan the narrow beam over large angles, the signal would have to be transmitting roughly ten times as long during each broadcast cycle.

#### D. APPLICATIONS

Due to the inefficiency in the generation of nonlinear parametric signals, the widespread use of parametric fog horns is not practical. It does provide a short range signal with reduced noise pollution that can convey more precise directional information and with scanning can warn the mariner of danger sectors to avoid or other geographical information.

### LIST OF REFERENCES

1. U.S. Environmental Protection Agency, "Information on Levels of Environmental Noise Requisite to Protect Public Health and Welfare with an Adequate Margin of Safety," 550/9-74-004, Washington, D.C. (1974).
2. Malme, C.I., "Development of Improved Baffle Systems for Directional Fog Signals," Bolt, Beranek, and Newman, Inc., Report 2991 for Contract DOT-CG-30200-A, U.S. Coast Guard (February 1975).
3. Shealy, W.P., "Parametric Difference-Frequency Generation of Sound in Air," Master's Thesis, Naval Postgraduate School, Monterey, California, December 1972.
4. Bennett, M.B., and Blackstock, D.T., "Parametric Array in Air," J. Acoust. Soc. Amer. 57, 562-568 (1975).
5. Brinkmann, Klaus, "The Interaction of Two Plane Sound Waves of Finite Amplitude and Coincident Direction of Propagation," Acustica 20, 92-100 (1968).
6. Moffett, M.B. and Mellen, R.H., "Model for Parametric Acoustic Source," J. Acoust. Soc. Amer. 61, 325-337 (1977).
7. General Requirements for Fog Signals, Title 33, Code of Federal Regulations, Chapter 1, Subpart 67.10.
8. Blaise, P., "The Definition and Method of Calculation of the Nominal Range and the Usual Range of a Sound Signal," International Association of Lighthouse Authorities, Supplement No. 3 (February 1969).
9. Westervelt, P.J., "Parametric Acoustic Array," J. Acoust. Soc. Amer. 35, 535-537 (1963).
10. Berkday, H.O. and Leahy, D.G., "Farfield Performance of Parametric Transmitters," J. Acoust. Soc. Amer. 55, 539-546 (1974).
11. Hixon, E.L. and Kuntz, H.L., "A Study of Broad Band High Level Audio Systems," Quarterly Progress Report for Contract DOT-66-63441-A, U.S. Coast Guard (January 1977).
12. Webster, D.A., Alexander, D.E., and Blackstock, D.T., "High Power Tests of the AEM Array," Supplement to E.L. Hixon and H.L. Kuntz, "A Study of Broad Band High Level Audio Systems," Quarterly Progress Report for Contract DOT-CG-63441-A, U.S. Coast Guard (October 1977).

13. Mellen, R.H., "Nearfield Axial Levels of Exponentially Shaded End-Fire Arrays," J. Acoust. Soc. Amer. 61, 559-602 (1977).
14. Rolleigh, R.L., "Difference Frequency Pressure Within the Interaction Region of a Parametric Array," J. Acoust. Soc. Amer. 58, 964-971 (1975).
15. Konrad, W.L., and Mellen, R.H., "The Parametric Array in Air," NUSC Tech. Memo. TD1Z-3-72, 12 June 1972.
16. Evans, L.B., H.E. Bass, and L.C. Sutherland, "Atmospheric Absorption of Sound: Theoretical Predictions," J. Acoust. Soc. Amer. 51, 1565-1575 (1972).

DISTRIBUTION LIST

	No. Copies
1. Defense Documentation Center Cameron Station Alexandria, Virginia 22314	2
2. Library, Code 0142 Naval Postgraduate School Monterey, California 93940	2
3. Commandant U.S. Coast Guard 400 7th St., S.W. Washington, D.C. 20590 Attn: Technical Library	1
4. Commandant U.S. Coast Guard 400 7th St., S.W. Washington, D.C. 20590 Attn: Ocean Engineering Branch	1
5. Commandant U.S. Coast Guard 400 7th St., S.W. Washington, D.C. 20590 Attn: Aids to Navigation Branch	1
6. Commander Coast Guard R&D Center Avery Point Groton, CT 06320 Attn: Physics Branch	1
7. Commander Coast Guard R&D Center Avery Point Groton, CT 06320 Attn: S.E. Trenchard	2
8. Officer in Charge Naval Underwater Systems Center New London Laboratory New London, CT 06320 Attn: M.B. Moffett	1

9. Officer in Charge 1  
Naval Underwater Systems Center  
New London Laboratory  
New London, CT 96320  
Attn: W.L. Konrad
10. The University of Texas at Austin 1  
Applied Research Laboratories  
Austin, Texas 78712  
Attn: M.B. Bennett
11. The University of Texas at Austin 1  
Applied Research Laboratories  
Austin, Texas 78712  
Attn: D.T. Blackstock
12. Director 1  
Naval Research Laboratory  
Department of the Navy  
Washington, D.C. 20390  
Attn: A.I. Eller
13. Department Library, Code 61 1  
Department of Physics and Chemistry  
Naval Postgraduate School  
Monterey, California 93940
14. Professor J.V. Sanders, Code 61Sd 1  
Department of Physics and Chemistry  
Naval Postgraduate School  
Monterey, California 93940
15. Professor A.B. Coppens, Code 61Cz 2  
Department of Physics and Chemistry  
Naval Postgraduate School  
Monterey, California 93940